NATIONAL ENERGY TECHNOLOGY LABORATORY

NETL

Natural Gas Hydrate Research

Award Number: Hydrates 2013.07.02
Project Period: October 1, 2013 – September 30, 2014

Quarterly Progress Report
Fiscal Year 2014, Quarter 2
January 1, 2014 – March 31, 2014

Yongkoo Seol, Technical Coordinator

U.S. DEPARTMENT OF ENERGY

List of Authors

Yongkoo Seol, ORD Technical Coordinator

Gary Sames, ORD Project Coordinator

George Guthrie, ORD Focus Area Lead

Jeffery Ilconich, RES Activity Manager

Table of Contents

List of Appendices

List of Figures

List of Tables

Acronym List

Acronym	Descriptive Name
ANS	Alaska North Slope
CMU	Carnegie Mellon University
CO_2	Carbon Dioxide
RHOB	Density
DOE	Department of Energy
DT	Sonic
FAL	Focus Area Lead
FEHM	Finite Element/Finite Volume Heat and Mass Transfer Computer Code
FPM	Federal Project Manager
FWP	Field Work Proposal
GR	Gamma Ray
GUI	Graphical User Interface
HQ	Headquarters
HRS	HydrateResSim
NETL	National Energy Technology Laboratory
ORD	Office of Research and Development
Pitt	University of Pittsburgh
PMP	Project Management Plan
PSU or Penn State	The Pennsylvania State University
R&D	Research and Development
Res	Resistivity
RES	Research and Engineering Services
RUA	Regional University Alliance
SARS	Safety Analysis and Review System
SCNGO	Strategic Center for Natural Gas and Oil
S_H	Hydrate Saturation
SHC	Shale Content
SOPO	Statement of Project Objectives
S_W	Water Saturation
TC	Technical Coordinator
THM	Thermal-hydrological-geomechanical
TM	Technology Manager
TMo	Technical Monitor
TVDSS	Total Vertical Depth
URS	URS Corporation

Acronym	Descriptive Name
VSHC	Volume of Shale Content
WVU	West Virginia University

1.0   Executive Summary

The National Energy Technology Laboratory (NETL) Office of Research and Development (ORD) supports the U.S. Department of Energy (DOE) National Gas Hydrate Research and Development (R&D) Program by providing numerical predictions on gas production activities and experimental estimations of physic-chemical reaction characteristics including geomechanical strength, gas exchange kinetics, and hydrate accumulation patterns in pore space. ORD's research will include combined efforts from the NETL-Regional University Alliance (RUA), Oak Ridge Alliance Universities – Oak Ridge Institute of Student Exchange (ORAU-ORISE), URS Corporation (URS), and URS subcontractors.

Continuing efforts on numerical simulations in Subtask 2.1 include history matching for the Iġnik Sikumi field test for the gas hydrate exchange trial using Mix3HydrateResSim. A series of reservoir simulations were performed to model the long-term response to depressurization. Laboratory experiments continued, particularly in the area of geomechanical reference tests to correct the rubber sleeve effect on mechanical strength measurements with hydrate-bearing sediments, and CO_2-CH_4 gas exchange kinetics with continuous flowing column setup. The two reference mechanical tests with rubber rods were used to derive the effect of a rubber sleeve, which were incorporated into the actual test. Maximum deviator stress increased with hydrate saturation when the saturation was higher than 30 percent, and elastic modulus showed the same pattern. An SMP subloading critical state constitutive model was developed and verified using the available data from the literature. Application of the model to the NETL test data is also in progress. Pore scale characterization of hydrate-bearing sediments using a micro CT scanner has been performed using analogue materials and pore network models have also been developed based on the 3D micro CT images.

This quarterly progress report provides the list of tasks, status of the work, major accomplishments, and updates regarding milestone dates. Research highlights this quarter include:

- Based on the Prudhoe Bay Unit, L-Pad hydrate-bearing sand deposit, a series of reservoir simulations and depressurization scenarios have been developed to model the response of a long-term depressurization test. The reservoir model has been generalized to two scenarios: (1) a fault-bounded system and (2) an anticline hydrate deposit. These will be used to simulate a depressurization test performed under varying conditions for temperature and depth.

- History-matching of the Iġnik Sikumi Field Trial have been conducted using Mix3HydrateResSim via the visualization tool, Petrasim. A simple 1-D CO_2 injection scenario has been developed using both a logarithmic (radial) system and a Cartesian system for distribution to Code Comparison Participants.

- After the calibration for the rubber sleeve effects, the results of NETL's geomechanical test on the non-cementing HBS samples were compared with other non-cementing HBS results by a Japanese group [1]. NETL's results, particularly compressive strength (max. deviator stress, q_{max}) data, appeared to be in good agreement with Japanese results.

- The modification of an acoustic sensor unit was completed and examined with the HBS sample. With the addition of a backing layer, the S-wave appeared distinguishable with resulting reductions in crystal ringing.

- A non-cementing hydrate formation test was completed for the inter-laboratory comparison study.

- An SMP subloading critical state constitutive model was developed and verified using the available data from the literature. Application of the model to the NETL test is also in progress.

- A laboratory-scale production test, using CO_2-CH_4 gas exchange technique, was performed for 500 hours. The cumulative recovery of the CH_4 from CO_2 and N_2, injected with CH_4-hydrate bearing sediments with the presence of free water, reached up to 35 percent, which is

significantly larger than the estimation from previous batch tests, but lower than expected based on literature value (up to 80 percent). The presence of free water in the pore space supports the lower than expected CH_4 recovery rates.

- An optimum parameter set for scanning hydrate-water-sand mixture with micro XCT 3D was identified from the CT scan with analogue samples, including plastics and corn oil. The current parameter set was derived from the images taken with the aluminum core holder and beryllium core holder, which provided better image quality due to the lower x-ray attenuation.

- Lattice pore network was developed to simulate the effect of hydrate habits and topology in pore space on hydraulic conductivity. The 3D pore network has also been extracted from micro CT images, based on rolling-ball algorithm.

References:

Ebinuma, T., Kamata, Y., Minagawa, H., Ohmura, R., Nagao, J. and Narita, H., "Mechanical Properties of Sandy Sediment Containing Methane Hydrate," Proceedings of the 5th International Conference on Gas Hydrates (ICGH 2005), Trondheim, Norway, June 12-16, 2005.

Masui, A, Haneda, H., Ogata, Y., and Aoki, K., "Effects of Methane Hydrate Formation on Shear Strength of Synthetic Methane Hydrate Sediments," Proceedings of the 15th International Offshore and Polar Engineering Conference, Seoul, Korea, June 19-24, 2005.

2.0   Goals and Objectives

The National Gas Hydrate Research and Development (R&D) Program has worked to accelerate the determination and realization of gas hydrate's resource potential and to better understand the role of gas hydrate in the environment. This Gas Hydrates Research project has been developed with a diverse set of research activities, performed by the U.S. DOE, NETL-ORD, and the RUA, to fill multiple needs within the National Gas Hydrate R&D program. The objective of the research project is to obtain pertinent, high-quality information on gas hydrates that will benefit the development of models and methods for predicting the behavior of gas hydrates in their natural environment under natural conditions and production scenarios. NETL-ORD supports major gas hydrate production field tests by providing numerical predictions on fluid migration, gas production, and potential reactions occurring during gas production activities; as well as, by providing fundamental understanding and knowledge on hydrate behavior derived from experimental investigations on thermal, hydrological, geomechanical, and reactive responses of hydrate. The proposed research consists of numerical modeling efforts, including:

- Simulations of long-term production tests and international code comparison studies for Iġnik Sikumi test

- Laboratory experimental tests on geomechanical measurements

- Gas exchange kinetics and mechanism tests

- High resolution visualizations of hydrate distributions in porous media

- General assistance and participation on domestic and international gas hydrate research and development activities

3.0   Technical Highlights, Results, and Discussion

The current progress of the work completed in FY14-Q2 is provided below. For each task and subtask, a detailed description is provided for the accomplishments this period, changes in approach, problems or delays, changes in key personnel, and technology transfer activities and products produced.

Task 1.0 Project Management and Outreach

This project is technically managed by the ORD Focus Area Lead (FAL). The FAL provides overall technical direction and guidance to the NETL-RUA research tasks. This project is implemented by a Technical Coordinator (TC) who provides the day-to-day technical and administrative management of the Field Work Proposal (FWP) tasks. Problems that arise during the execution of the various tasks will first be addressed by the TC, and if necessary the problem will be elevated to the attention of the FAL for resolution. If the support of the Strategic Center for Natural Gas and Oil (SCNGO) is needed to resolve any research issue, the FAL will do so during periodic meetings with the SCNGO Technology Manager (TM). Issues of a more administrative and reporting nature will be resolved with the FWP Technical Monitor (TMo).

Accomplishments this Period:

The project management activity produces internal and public reports required to demonstrate competent technical and administrative execution of the project. Deliverables submitted and accomplishments met during this activity period are as follows:

- The FY14-Q1 report was submitted to SCNGO on January 31, 2014.
- Regular monthly task and subtask level group meetings were conducted among DOE, URS, and NETL-RUA personnel.
- Monthly invoice reviews were conducted prior to the ORD approval of the invoices.
- Milestone and deliverable status were monitored and updated.

Changes in Approach:

Nothing to report during this activity period.

Problems or Delays:

Nothing to report during this activity period.

Changes in Key Personnel and Partnerships:

Nothing to report during this activity period.

Technology Transfer Activities or Product Produced:

Nothing to report during this activity period.

Task 2.0 Reservoir Simulation of Gas Hydrates Production Field Tests

Objectives

- Provide modeling predictions utilizing current capabilities for past and future potential field tests, including a long-term depressurization test on the ANS and the ConocoPhillips CO_2-CH_4 exchange test. Modeling results will be compared with available field data.
- Coordinate an international effort for the analysis of the Iġnik Sikumi CO_2-CH_4 exchange test and cross-validation of the participating reservoir simulation codes using test data sets and data from the Iġnik Sikumi test.

Scope of Work

Simulations of field tests in the ANS are designed to test the efficacy of using depressurization and CO_2 injection as a means to initiate gas production from Arctic hydrate deposits below the permafrost. The

short-term goal of this task is to provide modeling predictions for future potential field tests (e.g., long-term depressurization test) and to analyze and extrapolate longer-term responses from recent field tests (e.g., ConocoPhillips CO_2-CH_4 exchange test).

Accomplishments this Period:

Subtask 2.1 Simulations of Long-Term Production Scenarios: Depressurization and CO_2 Exchange

Various reservoir simulation scenarios, modeled after the Prudhoe Bay L-Pad hydrate-bearing sands as well as, 2D simulation scenarios modeled after the Mount Elbert deposit for various Site 2 temperatures and depths, have been performed. A full 3D realization of the Mount Elbert deposit has also been constructed. In the coming months, work with the DOE and USGS to identify sites for future test simulations will continue.

Dipping Structure, Fault-Bounded Up Dip (Similar to PBU L-Pad)

The model shown in Figure 1 was built from a 5 ft interval contour data, available from USGS, and is an extracted sub model from a parent model shown in Figure 2. The model is bounded in the west by a system of vertical faults, which almost form a three-way closure and in the east by the hydrate-water contact at 685 m (2,248 ft). The northern and southern boundaries were chosen as guided by the fault system in the west boundary.

The sub model grid measures 950 x 1,800 x 45 m and is divided into 30 x 50 x 80 simulation grid blocks in the x, y, and z directions, respectively.

Due to the complexity of the hydrate dissociation process, grid refinements were completed in the region of high hydrate saturations and also in regions near the wellbore. These were done such that the effective radius of the wellbore grid was 0.6 m (smallest possible, to guarantee simulation convergence for this system) and the thickness of the high hydrate saturation layers was 0.43 m, while other layers had a thickness of 0.87 m.
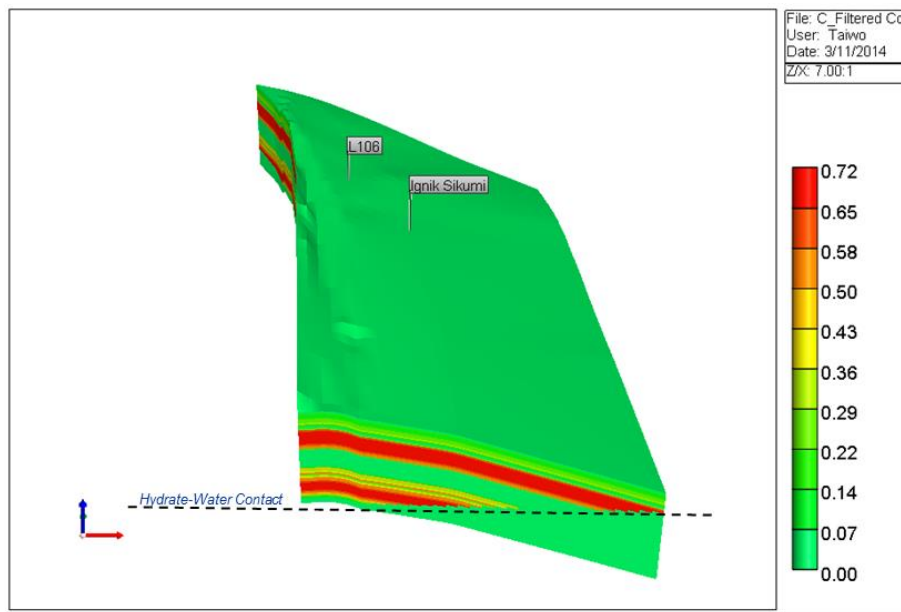
Figure 1: Extracted sub model showing initial hydrate distribution and hydrate water contact.

Original Reservoir 3D Structure

Extracted Submodel of the Target Area
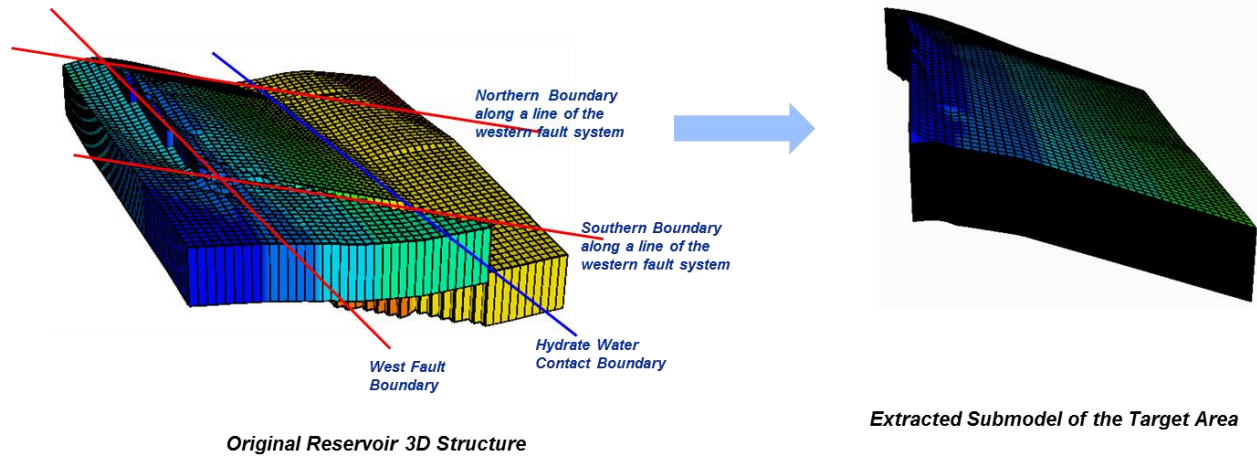
Figure 2: Extracted model of the target area.

Models were run for different scenarios with L-106, Iġnik Sikumi, and dummy wells Well-1 and Well-2 with only one well producing for each scenario. Well-1 is a vertical well down dip of Iġnik Sikumi and Well-2 is a deviated well which penetrates the C1 sand further down dip on the Prudhoe Bay L-Pad. Figure 3(a) through (c) are the vertical cross sections of the model showing the locations of each of these wells.
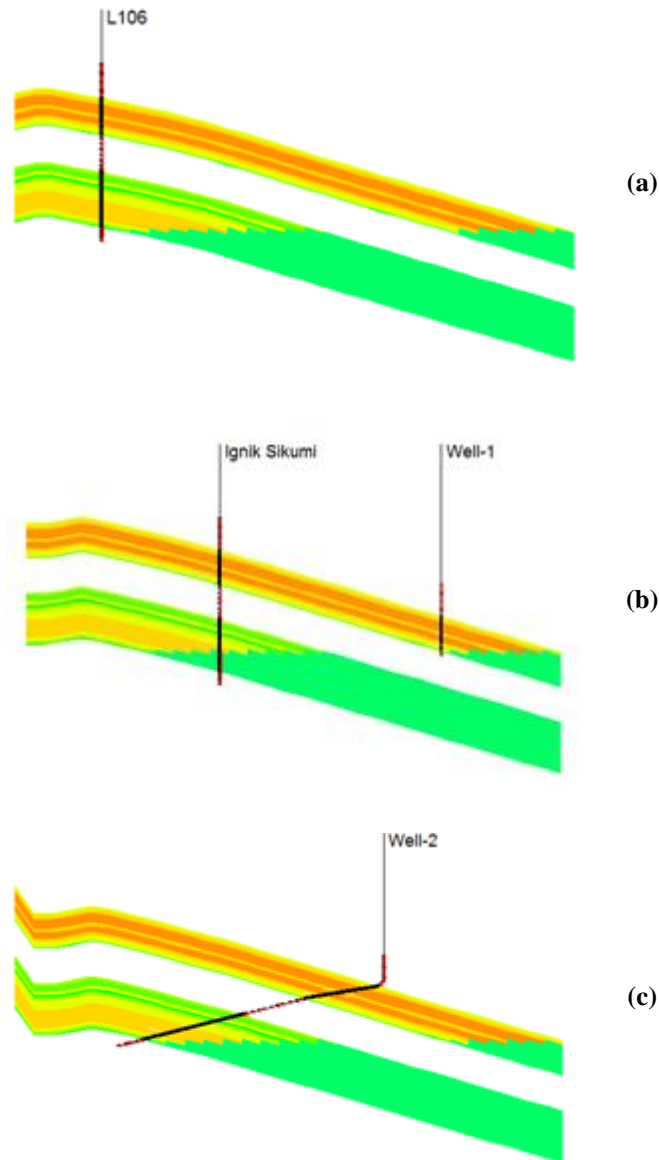
Figure 3: Vertical cross sections of the model with wells.

Simulation Results and Discussions

Comparison of the gas production rate profiles is shown in Figure 4. A significantly higher gas rate is observed for the deviated Well-2 as expected because it has the highest hydrate contact and penetrates the C sands in the deepest and warmest part of the reservoir. At the end of the fifth year, 48,000, 19,400, 19,000, and 17,450 m^3/day of gas production was achieved for Well-2, Iġnik Sikumi, L-106 and Well-1.

The initial rate was higher in L-106 than Iġnik Sikumi and Well-1. This was because, in the early stages of testing, the L-106 had more contact with hydrate and so initially, more gas was produced in L-106 than Iġnik Sikumi and Well-1.

After a while, the contribution of gas from the C2 sand vanished and the effect of the warmer C1 sands tended to become more prominent in Iġnik Sikumi and Well-1. This was also explained by the change in hydrate saturation distribution with time, as presented in Figure 5, for L-106 and Iġnik Sikumi.

Overall, the results showed that the gas production rate was not only a function of the depth (temperature) of formation but of how much hydrate was in contact with the producing wells.
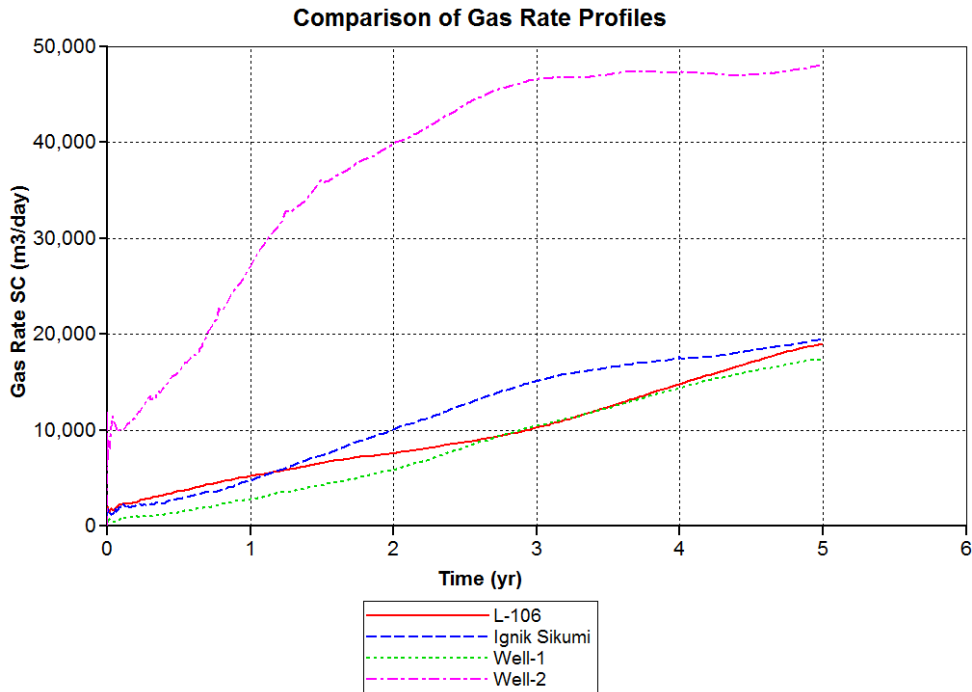
Figure 4: Gas rate profiles.
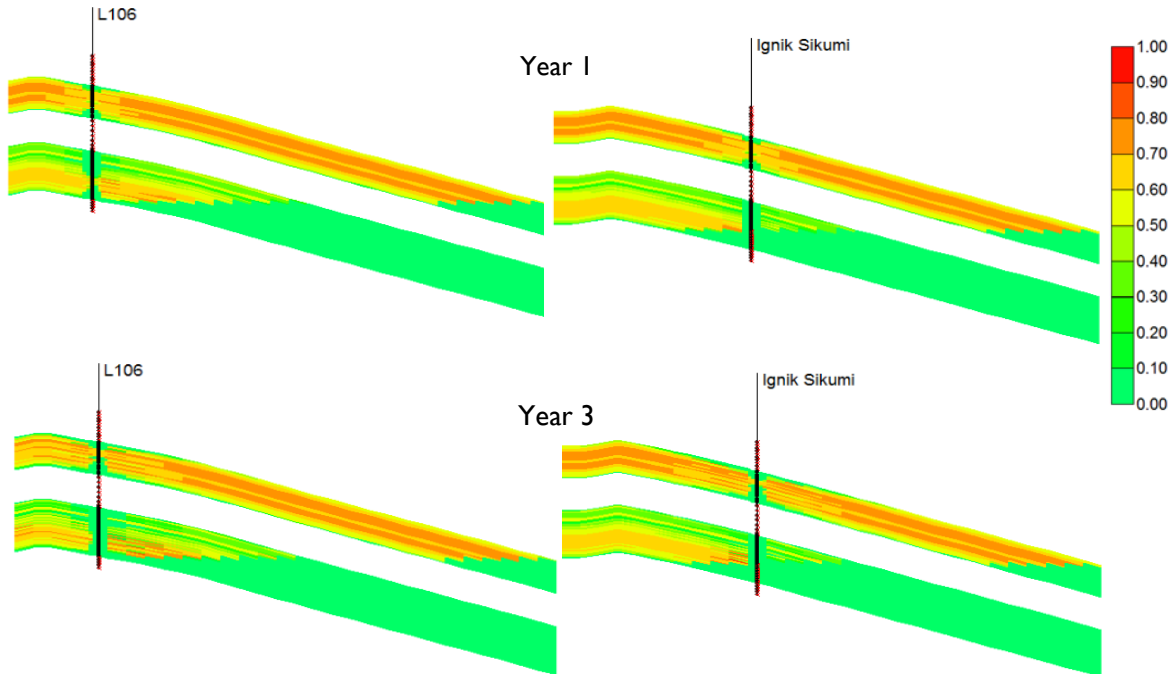
Figure 5: Vertical variation of hydrate saturation distribution with time.

The gradual expansion of the hydrate dissociation front away from the wellbore was noticeable. It was observed that C2 dissociates more readily than C1. At the end of the first year, the L106 well was still producing from the C2 sand, which supports the earlier explanation of the initial higher rates observed from L106.

Fault-Block Structure for Site 2 Evaluation (Similar to Mount Elbert)

Model Description

The Site model is a deeper (hence warmer) version of the 2D Mount Elbert Model. As shown in Figure 6, the grid structure was essentially the same as that of Problem 7a. It was a cylindrical grid system with a vertical production well at the axis of the cylinder. There were 80 cells distributed logarithmically along the wellbore radius (r_w) = 0.111m to r = 450 m.

A total of 50 cells, each having a thickness of 0.25 m, represented the hydrate-bearing layers of the model. Each of the overburden and underburden shale had a division of 10 layers with thicknesses ranging from 0.25 m to 70 m from center to periphery as defined by the equation $dz_i = 1.694831 dz_{i-1}$.
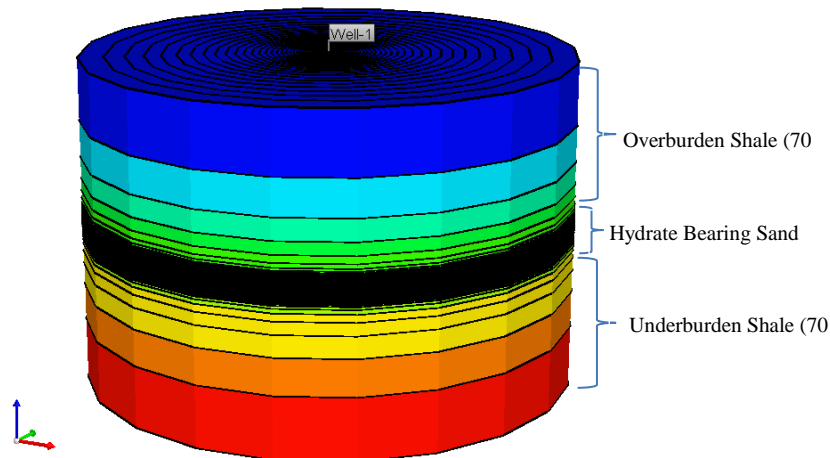
Figure 6: Cylindrical grid structure of Site 2.

Since the depth of hydrate formation in Site 2 is not yet known, various models with different depths (to the top of hydrate formation) were run for 620, 670, 720, and 770 m.

Corresponding pressure and temperature variation in the grid were linearly extrapolated from the 2D Mount Elbert model using an average pressure gradient of 9.98 kPa/m and a temperature gradient of 0.036 K/m.

Temperature ranges for each of the models were:

- 620 m (5.2 – 5.6°C)
- 670 m (7.0 – 7.4°C)
- 720 m (8.8 – 9.2°C)
- 770 m (10.6 – 11.0°C)

Each of these models was run starting with a well bottom-hole pressure of 4,160 kPa and then decreased gradually to 2,700 kPa just as in Problem 7a.

Simulation Results

Gas rate profiles of these models were plotted and compared to that of the 2D Mount Elbert model as shown in Figure 7.

As expected, higher gas rates were achieved with an increase in depth (temperatures), with peaks at 88,428, 62,560, 37,990, and 22,750 m^3/day, respectively. This suggests that Site 2 may be a more favorable production site than the Prudhoe L-Pad, in terms of gas recovery potential only. It was also observed that peaks were reached early in the warmer models compared to the colder ones.

Comparison of Gas Rate Profiles at Various Depths
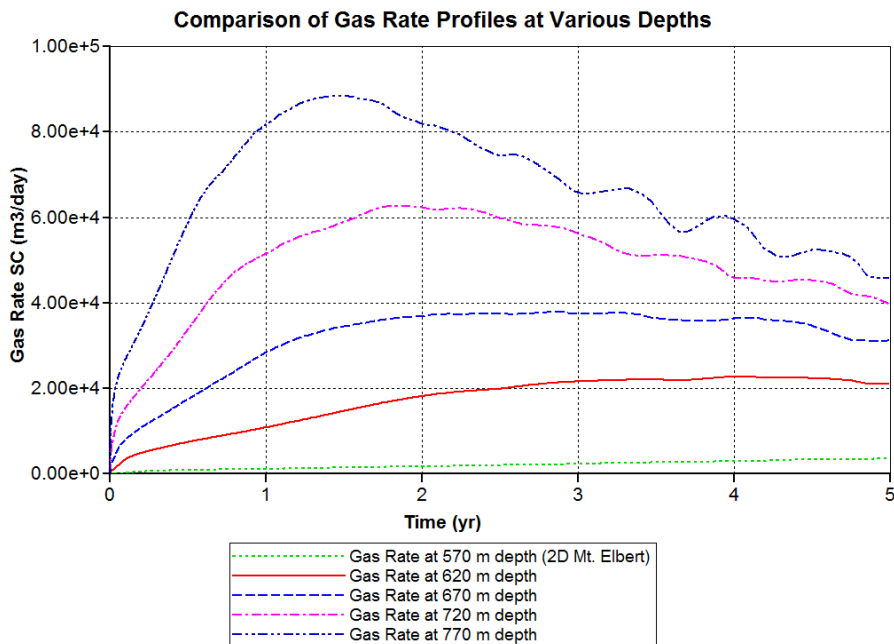
Figure 7: Site 2 gas rates at different depths (to top of HBS).

Subtask 2.2 International Code Comparison Problem Set Based on Iġnik Sikumi

Problems developed for the international code comparison:

Problem 1

A horizontal, 1D domain 20 m in length was considered in which only a water-CO_2 system was considered in the entire domain. The main objective of this problem was to study the mass and heat flow in a porous media in a 1D domain consisting of a CO_2-water system. It was a two-component, two-phase system. Physical and hydrological parameters of the domain are listed in Table 1 and Table 2. High pressure, temperature gradients and complete aqueous saturation conditions were specified in the first 10 blocks, and aqueous unsaturated conditions in the next 10 blocks. As the simulation proceeded, equilibrium conditions were reached in the entire domain due to mass and heat flow in the domain.

The schematic of the domain used is shown in Figure 8. Considering *x* as the horizontal distance, the pressure and temperature at three different locations (*x*=0, 10, 20 m) were specified. The same properties for other blocks were calculated based on their gradients in the horizontal direction.

Absolute permeability used was 1,000 mD.

P=5 MPa	*P*=4.8 MPa	*P*=4.6 MPa
T=5 °C	*T*=15 °C	*T*=25 °C
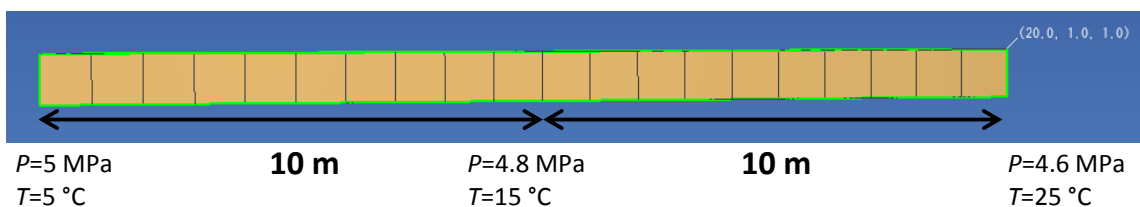
Figure 8: One dimensional domain considered for Problem 1.

Table 1: Parameters Used in Problem 1

Parameters	Value Used
Porosity	0.3
Density	02650 Kg/m^3
Thermal Conductivity	2.0 W/m K
Specific Heat	750 J/kg K
Pore Compressibility	5.0×10^{-10} Pa^{-1}

Table 2: Parameters for Relative Permeability and Capillary Pressure Functions

Relative Permeability	Aziz and Stone Equation
S_{irA}	0.15
S_{irG}	0.05
n	3
Capillary Pressure	**Van Genuchten Function**
S_{irA}	0.14
n	1.84
α	10

Results

The profiles of aqueous saturation, temperature, and pressure of the domain are obtained for different time steps (in Figure 9, the profiles are shown for 1 day, 10 days, 100 days and 1,000 days).
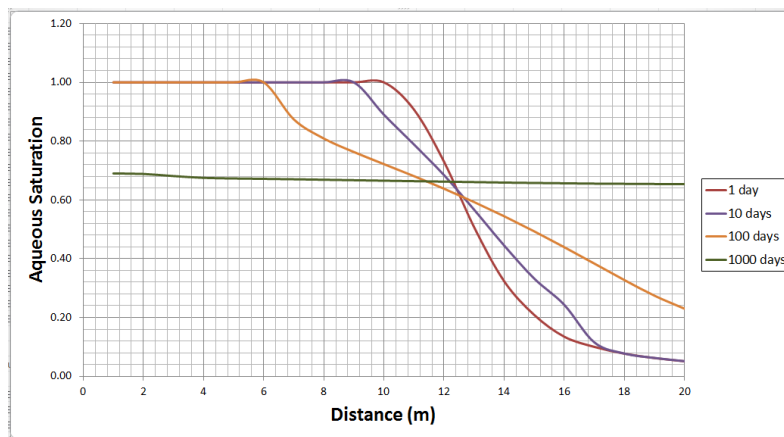
Figure 9: Aqueous saturation profiles at different time steps.
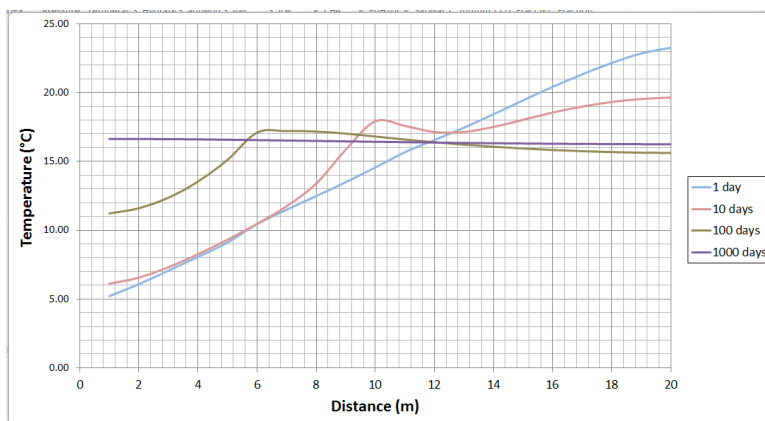
Figure 10: Temperature profile at different time steps.

Discussion

As per the problem description, there is only aqueous phase present in the first half of the domain and unsaturated conditions (Aq and G phases) are considered in the second half. Over the period of time, due to mass transfer, water flowed from one part to the other. As shown in Figure 9, by the thousandth day, aqueous saturation of the entire domain reached nearly 0.7 and hence, equilibrium is believed to have been reached in the reservoir. This reasoning also applies to temperature change in the reservoir. Due to heat transfer, thermal equilibrium is reached by the thousandth day, which is fortified by the Figure 10, in which the temperature of the entire domain is at 16.8°C.

Problem 2

This problem uses the same grid as Problem 1. The major difference between these two problems is that here in the first half of the domain hydrate phase is considered (Figure 11). Hydrate dissociates mainly due to thermal stimulation provided from the second half of the domain. The hydrate dissociation is simulated using an equilibrium model. The system used in this model is water-CO_2-hydrate.It is a three component, three phase system.
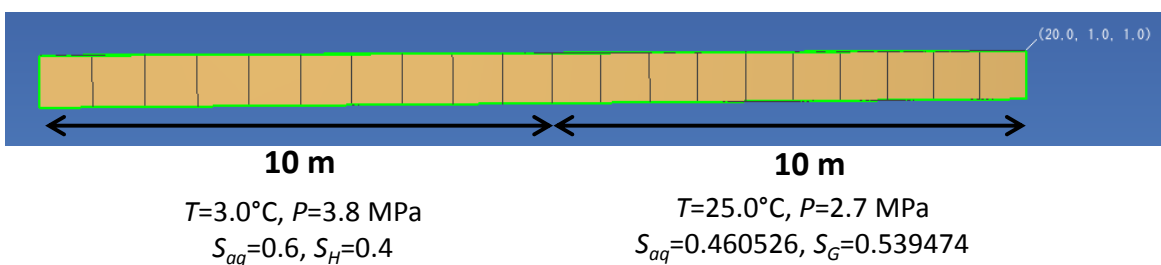
Figure 11: Schematic diagram used for Problem 2.

The parameters used in Problem 2 are the same as that of Problem 1 listed in Table 1 and Table 2.

Results and Discussion

Initially, thermal stimulation and depressurization caused hydrates to dissociate, but later in the testing, thermal stimulation was the only cause for hydrate dissociation (Figures 12 through 14). Hydrate formation was observed after 100 days (see Figure 14) along with dissociation due to the movement of released CO_2 gas from the other half of the domain. As shown in Figure 15

(temperature profiles), from the thousandth day, the temperature remained constant in the entire domain, but from saturation figures it is evident that the hydrate in the domain did not dissociate completely. In the first half of the domain, AGH phase was observed. As Mix3hydrateResSim assumes that the hydrate is a ternary hydrate in the reservoir, trace amounts of CH_4 and N_2 hydrate formations may also take place.
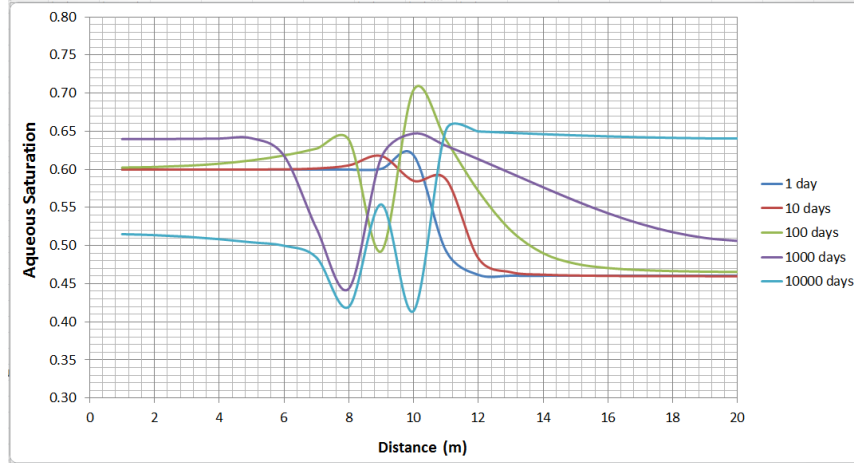
Figure 12: S_{aq} profiles for different time steps.
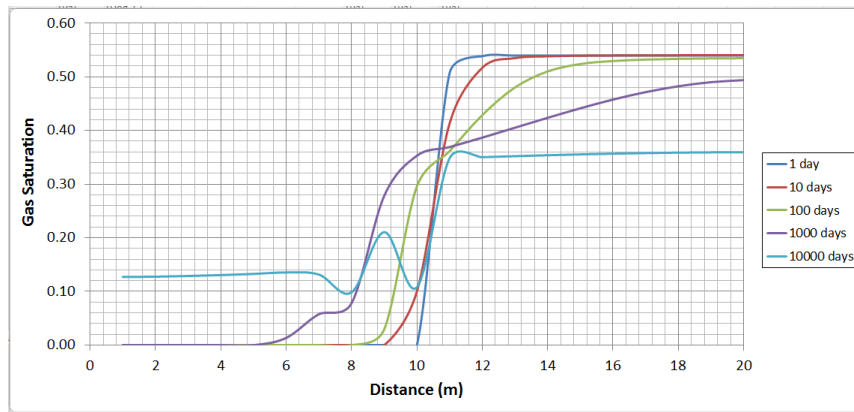
Figure 13: S_G profiles over the period of time.
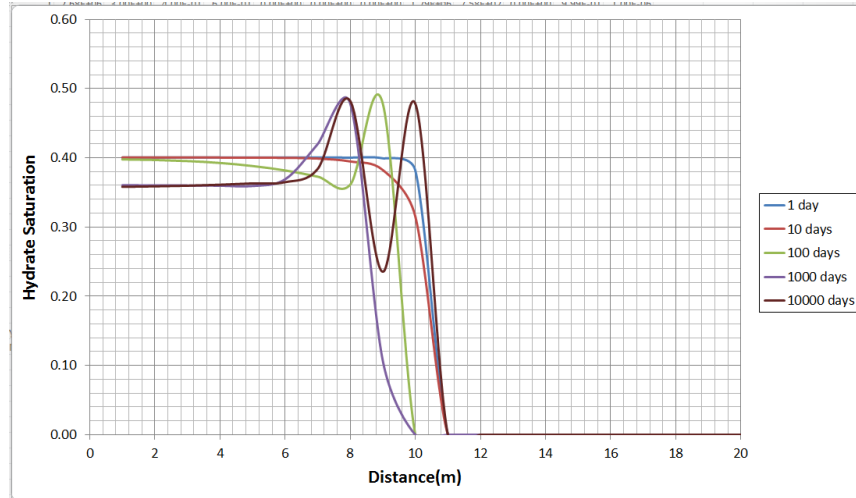
Figure 14: S_H profiles at different times.
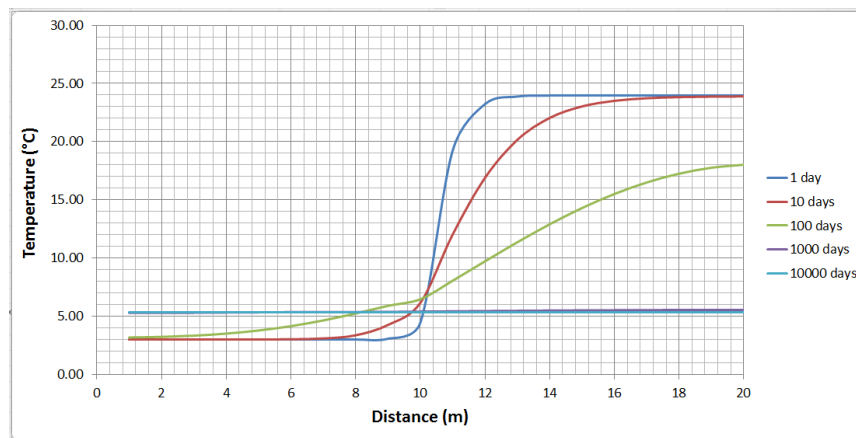
Figure 15: Temperature profiles at different times.

Changes in Approach:

For Subtask 2.1, a contingency approach to simulation sites has been taken. The exact location of a potential long-term depressurization test site is yet to be determined, and thus simulations of the Prudhoe Bay L-Pad hydrate-bearing sands have proceeded. These simulations will be quickly adaptable to other test sites as identified.

Problems or Delays:

Nothing to report during this activity period.

Changes in Key Personnel and Partnerships:

Nothing to report during this activity period.

Technology Transfer Activities or Product Produced:

Nothing to report during this activity period.

Task 3.0 Developing Constitutive Models of Various Hydrate-Bearing Sands

Objectives

This task will fulfill two objectives:

1. Develop constitutive models for various hydrate-bearing sediments under in situ overburden pressure and temperature conditions.

2. Provide a rational basis for modeling and predicting the geomechanical behavior and stability of hydrate-bearing sands in the field during gas production (using depressurization and gas exchange). The results of this task will aid in understanding the behavior of hydrate-bearing sediments under gas production and will provide insight that will assist in optimizing the design of future production operations.

Scope of Work

This work will implement and test the constitutive laws of the hydrate-bearing sands developed in FY13 based upon NETL laboratory tests. The constitutive law will be utilized to predict the geomechanical behavior of hydrate-bearing sediments under gas production (dissociation or gas exchange). Additional laboratory tests will be performed to measure mechanical parameters of the sediments with various conditions such as binary hydrate mixtures during gas exchange process. The constitutive law will be implemented into a geomechanical analysis code, and this code will work with a multiphase flow code.

Accomplishments this Period:

Sub-subtask 3.1 Laboratory Measurements of Geomechanical Strength and Deformability

The results of the geomechanical test on the non-cementing HBS samples, calibrated for the rubber sleeve effects, have been compared with other non-cementing HBS results, particularly by Japanese group in this report. As shown in Figure 16 (as an example), our compressive strength (max. deviator stress, q_{max}) data are generally in good agreement with Japanese results, by following the trend of strength variation with the effective confining stress (σ'_3) in the range of 0.69 to 3 MPa. Both data also show that the q_{max} increases with the σ'_3, and no significant increases in q_{max} below the hydrate saturation (S_h) of ~30%, which corresponds to the point where the hydrate formation habit changes from pore-filling to load-bearing. More comparison works are currently being conducted with similar experimental results from other research groups.
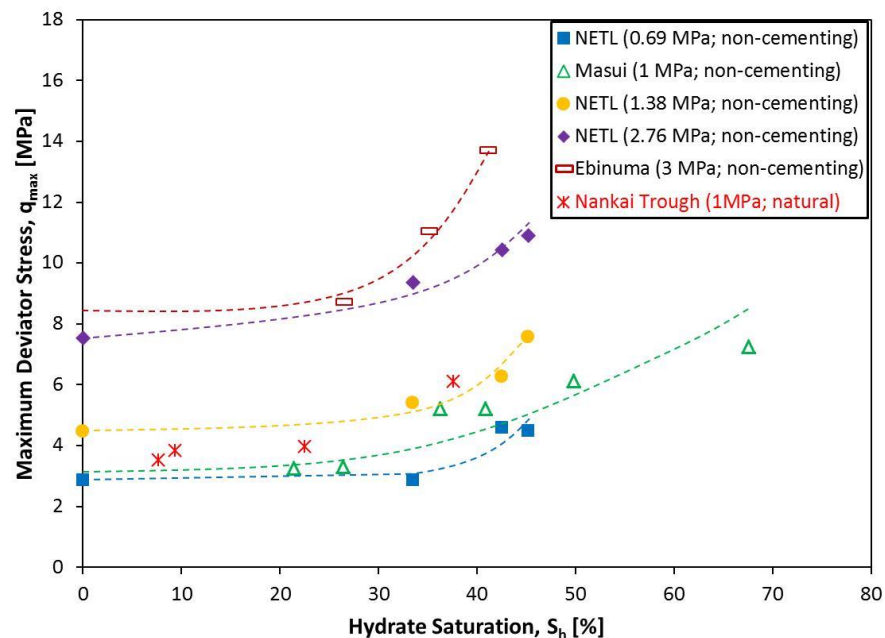
Figure 16: Maximum deviator stress versus hydrate saturation at various non-cementing hydrate saturations (comparison between NETL and Japanese data).

The modification of the acoustic sensor unit has been completed and examined with the HBS sample. A backing layer, made of mixture of tungsten powder and epoxy, was attached on top of each of P- and S-wave crystals for damping and attenuation of ringing in the crystal (Figure 17). The influence of adding a backing layer is pronounced particularly for S-wave signal. With the backing layer, the S-wave can be distinguishable with its noticeably large amplitude (Figure 18). The precursor of P-wave that always arrives first preceding the S-wave was also noticed. This P-wave precursor possibly occurred due to the imperfect polarization of S-sensor in the radial direction. Figure 19 confirms that the first arriving wave detected by the S-crystal is P-wave; the arrival time of the precursor wave, detected by S-crystal, matched that of the P-wave detected by P-crystal. Wave analyses are being conducted to investigate the variation of P- and S-wave velocity during hydrate formation habit change, as a part of an inter-laboratory study with USGS and CSM.
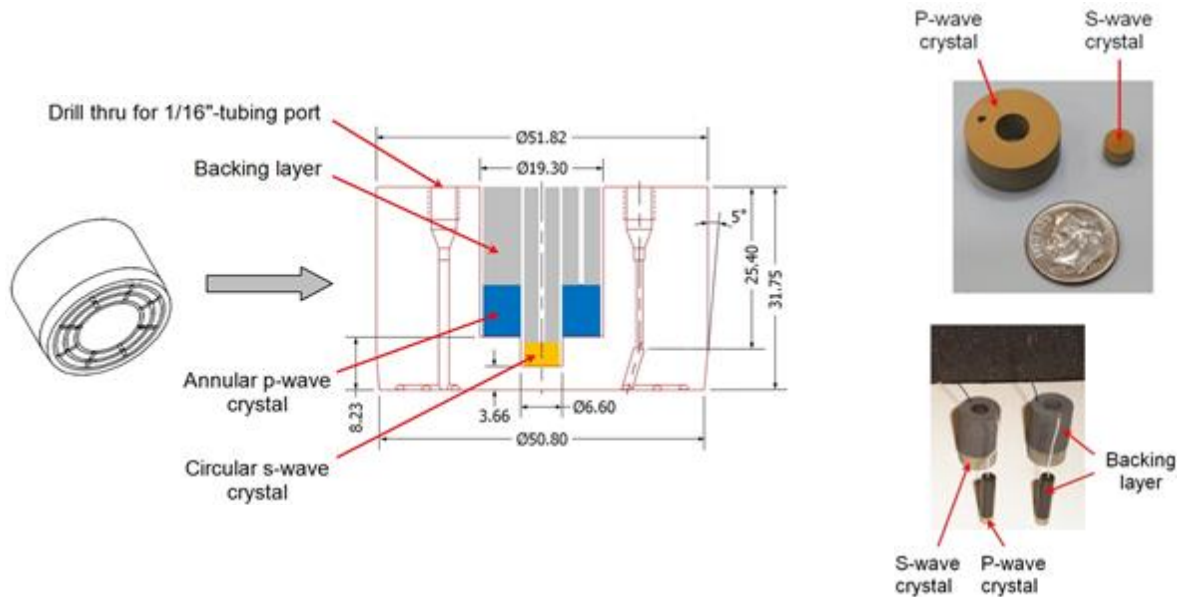
Figure 17: Acoustic sensor unit modified with adding backing layers.
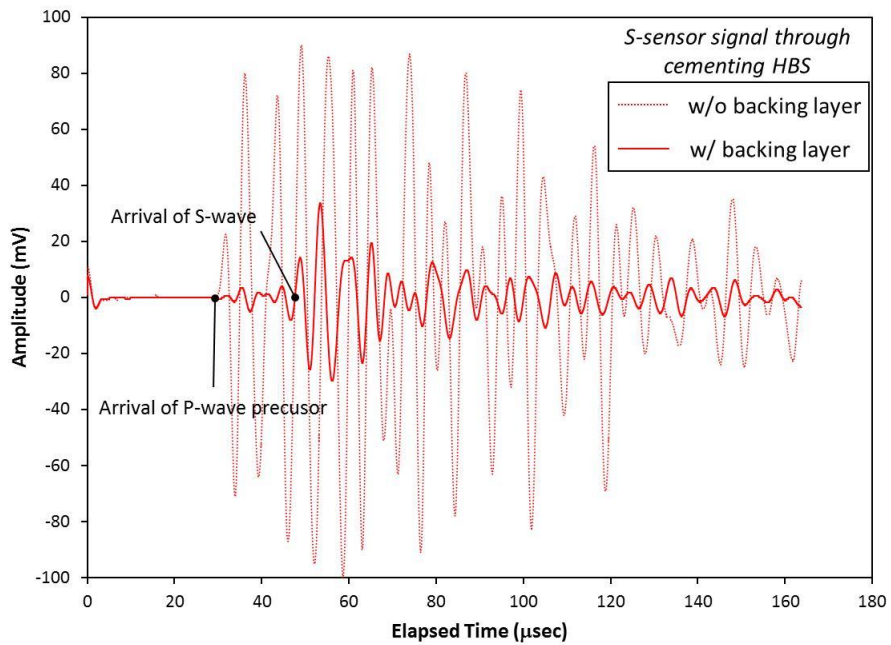
Figure 18: Comparison of S-waveforms without and with backing layer for cementing HBS samples (S_h = ~ 45-56%).
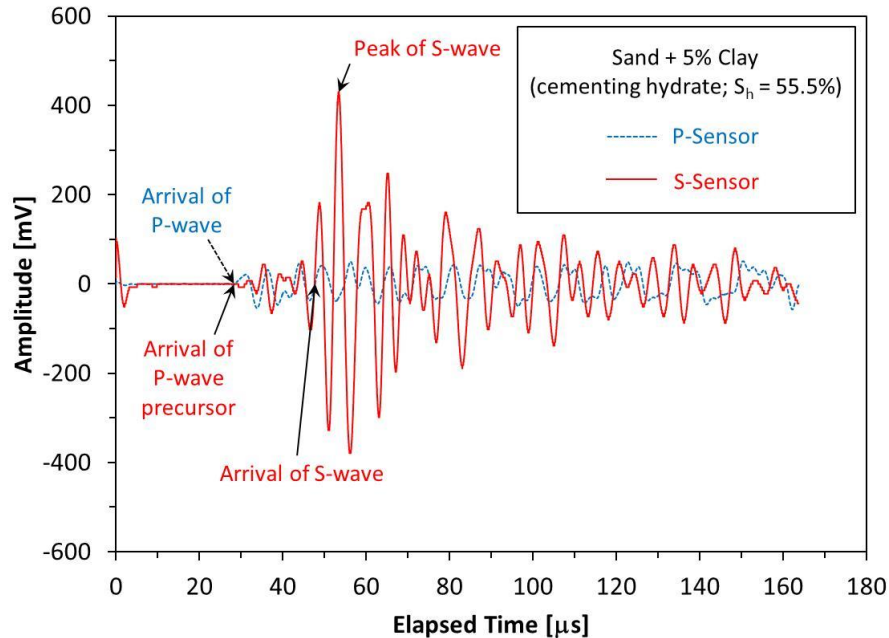
Figure 19: P- and S-waveforms measured by modified acoustic unit with backing layer for cementing HBS samples (S_h = ~56%).

Subtask 3.2 Developing Constitutive Models of Various Hydrate-Bearing Sands

After successfully demonstrated that the proposed SMP model was capable of describing the behavior of sands and methane hydrate bearing soils, the research moved on to incorporate it into a geomechanics code. For this, we have implemented a dynamic link library for the commercial code FLAC3D. A first version of the implementation was accomplished. More testing is underway.

The implementation was carried out for FLAC3D 4.0, which requires the use of Visual C++2005. The input data required are: the Poisson Ratio, kappa, lambda for the isotropic consolidation, the pre-consolidation pressure, Pcs. The known point on the Normal consolidation line was p1 for pressure, and mV1 for the specific volume.

SMP model specific input included, beta=2 for sands; the critical state parameter defined by RS; the u parameter for subloading model was 7.2 (smp_u). For the Hydrates, input included Sh for hydrate saturation defined as smp_sh; the increased yield strength is Xpcd=a (Sh^b); with Sh=psi*Sh; and psi was degrading as a function of the plastic strain governed by m. Parameters coded were smp_a; smp_b; smp_m.

For loading, the input included the confining pressure and loading rate.

In this report, two simulated triaxial tests results are shown, both using one soil element; one run was for sand (Figure 20), the other for methane hydrate bearing soils (Figure 21). For sands, the parameters used are as follows: poisson = 0.2, kappa = 0.05, lambda = 0.2, Beta = 2, m = 1, MV1 = 2.3, maximum past pressure = 8, RS = 3.2, xMP = 1.

For the hydrate bearing sands, the run used the following parameters: poisson = 0.2, kappa = 0.004, lambda = 0.16, Beta = 2, Sh = 0.2, smp_a = 40, smp_b = 1, smp_m = 3, smp_u = 7.2, mv1 = 2.42. Pcs = 2000, RS = 2.75, xMP = 198.
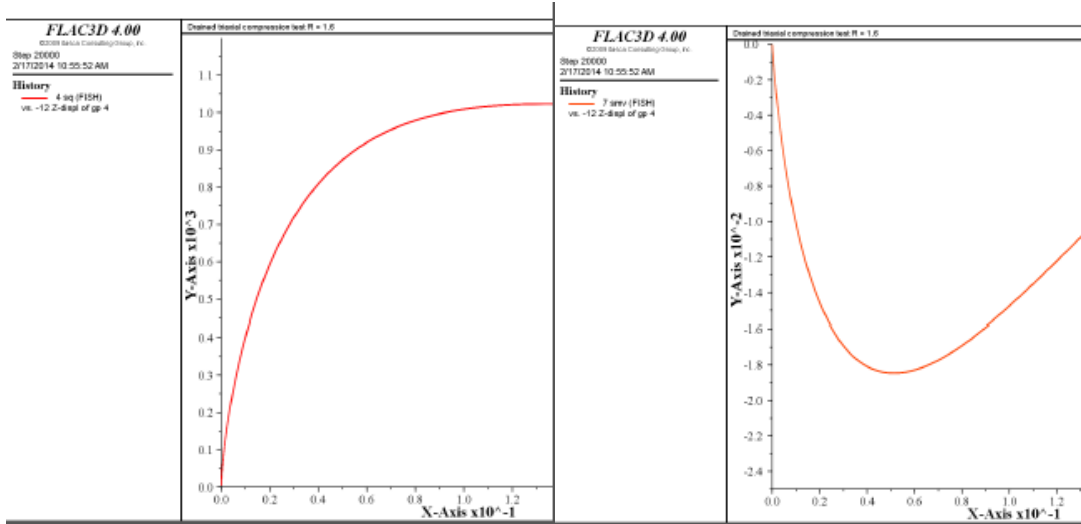
Figure 20: Flac3D runs with SMP soil model for sands.
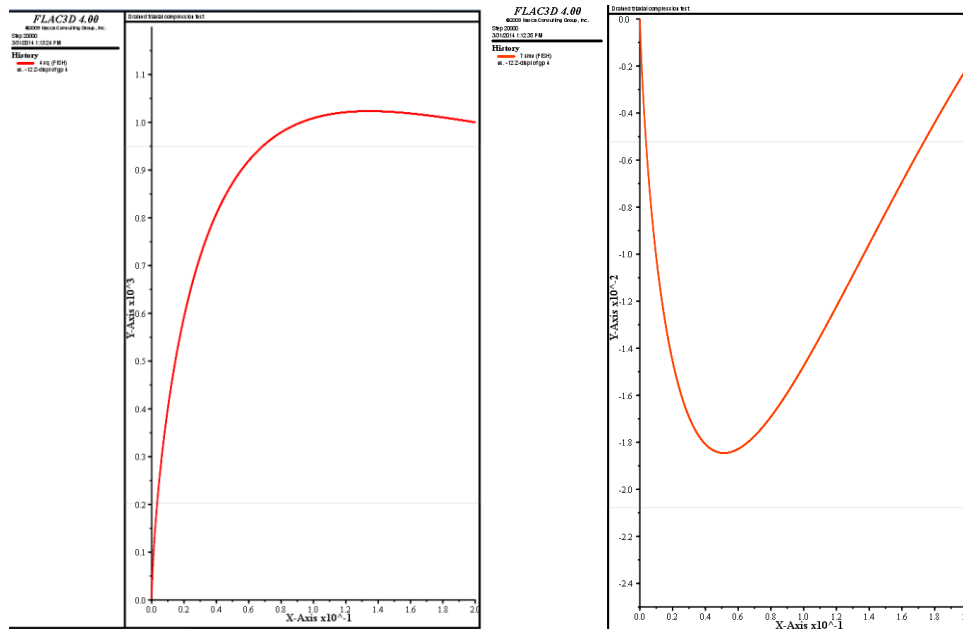
Figure 21: Flac3D runs with SMP soil model for hydrate bearing sands.

Tests on soil bearing tetrahydrofuran hydrate from Georgia Tech have also been considered. It was concluded that at some point when hydrate saturation becomes exceedingly high, the material properties may no longer have soil characteristics. The soil characteristics could be modeled with S_H up to about 50%, but not when S_H reaches 100%.

Changes in Approach:

Nothing to report during this activity period.

Problems or Delays:

Nothing to report during this activity period.

Changes in Key Personnel and Partnerships:

Nothing to report during this activity period.

Technology Transfer Activities or Product Produced:

Choi, J.-H., Dai, S., Cha, J.-H., and Seol, Y., "Laboratory Formation of Non-Cementing Hydrates in Sandy Sediments," journal paper, accepted by *Geochemistry, Geophysics, Geosystems*.

Seol, Y., Choi, J.-H., and Dai, S., "Multi-Properties Characterization Chamber for Hydrate Bearing Sediments," draft paper, under internal review for possible publication in *Review of Scientific Instruments*.

Task 4.0 Assessment of Gas Exchange Processes of CH_4 Hydrate with CO_2 under Reservoir Conditions

Objectives

- Determine the mechanisms of gas exchange between CO_2 and CH_4 when CO_2 is injected into CH_4-hydrate-bearing sediment for CH_4 production.

- Determine the kinetics of gas exchange in the systems with the presence of free water and varied gas mixtures (CO_2, CH_4, and N_2) within pore space.

- Share/exchange gas exchange kinetics data with LBNL and PNNL for comparative analysis of exchange kinetics data acquired under different reaction conditions.

- Utilize experimental results to enhance understanding of gas exchange processes as a gas production technology and help identify optimum conditions (such as composition of feed gas and pore gas and free water saturation) for sustained CH_4 production.

Scope of Work

The mechanisms of replacement of CH_4 with CO_2, within a system containing CH_4 hydrate, will be experimentally assessed using Raman spectroscopy. Experimental tests will be continued which focus on measuring the replacement kinetics in both the batch and column systems, where CO_2 or CO_2 and N_2 mixed gas will be injected in the presence of free water. It is also planned to share/exchange the resultant gas exchange kinetics data with LBNL and PNNL for comparative analysis.

Accomplishments this Period:

Subtask 4.1 Gas Exchange Mechanism with Raman Spectroscopy

Nothing to report during this activity period.

Subtask 4.2 Gas Exchange Kinetics Measurements in the Presence of Free Water

Liquid CO_2-CH_4 Exchange Kinetics in Batch Mode

Procedures

The sand measured at 52.9 g moistened with water measured at 4.9 g was packed into a high pressure vessel to yield the porosity of 36 percent and water saturation (S_W) of 45 percent in pore space. The methane hydrate coexisting with free water was obtained by the procedures reported previously (see FY14-Q1 report). The mass balance calculation demonstrates the hydrate

saturation (S_H) of 33 percent and free water saturation (S_{FW}) of 14 percent. CO_2 gas was injected into the reactor under constant flow rate mode of 15 ml/min while the pressure in the reactor was maintained at 3.59 MPa at 1°C, respectively, to allow the removal of CH_4 gas in head and pore spaces. When the composition of CH_4 in the gas flow coming out of the reactor became lower than 2 percent, CO_2 was further pressurized to 5.4 MPa to create CO_2 (l) stable condition. The gas composition in gas phase was measured by using a Shimadzu DS2014 gas chromatograph with a TCD detector and He carrier gas.

Results

The gas exchange test was carried out by injecting liquid CO_2 into methane hydrate bearing sediment (MHBS) with S_H of 33 percent and S_{FW} of 14 percent at 5.4 MPa and 1°C. When CO_2 (l) is injected into the MHBS, CH_4 gas released from methane hydrate (MH) would not be mixed with CO_2 (l) readily and uniformly, and the effluent fluid stream may not represent the average composition of mobile phase within pore space. Therefore, the exchange efficiency and gas recovery rate for this CO_2 (l) + CH_4 system was estimated based on gas composition analyzed for the gas in the effluent collection pump after gas exchange process has been completed. The CH_4 recovery rate reached at 52 percent after 717 hours from the beginning of exchange process (Figure 22). The CH_4 recovery rate of the CO_2 (l) injection system with free water presented much higher value compared to CO_2 (g) injection system with free water and similar to the CO_2 (g) system without free water.

Liquid CO_2-CH_4 Exchange Kinetics in Column Mode

The batch test on liquid CO_2 injection may be more promising as CH_4 recovery rate becomes higher in the presence of free water compared to (CO_2 + N_2) mixed gas injection system. Thus, the focus will be more on CO_2 (l)-CH_4 gas exchange system to efficiently produce CH_4 gas from natural hydrate reservoirs. The plan in FY14 is to test the gas exchange kinetics in high S_H condition. A high S_H sand sample was prepared by the procedure which was reported in a recent publication [1]. However, high S_H would incur undesirable hydrate formation from free water, which plugs the pathway of feed gas and prevents the contact between methane hydrate and feed gas. Use of warm liquid CO_2 injection is suggested to avoid CO_2 hydrate formation condition while methane hydrate keeps stable (Figure 23). At this condition, dense liquid CO_2 phase could push free water toward outlet stream and removed it from pore space. Thus, the availability of methane hydrate for liquid CO_2 will increase. When the brine replacement step is completed, the injection of warm CO_2 will be stopped, whereas cooled CO_2 will be supplied into the reactor. Thus, liquid CO_2 enters the condition where CO_2 (l)-CH_4 exchange occurs in methane hydrate phase.
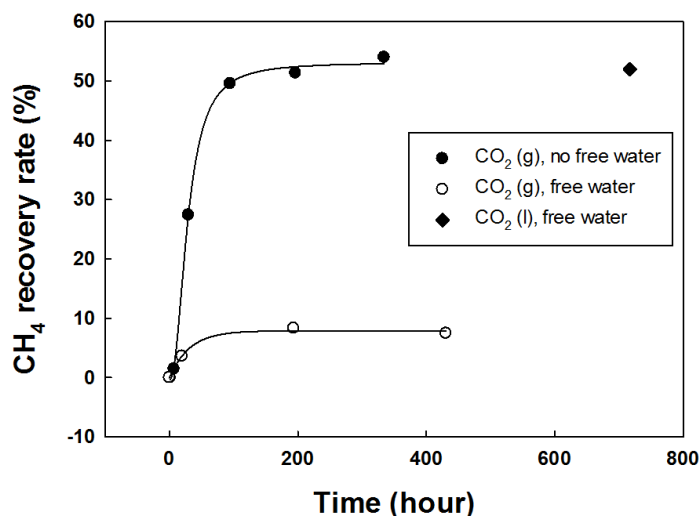
Figure 22: CH$_4$ recovery rate in CO$_2$-CH$_4$ gas exchange system in batch mode.
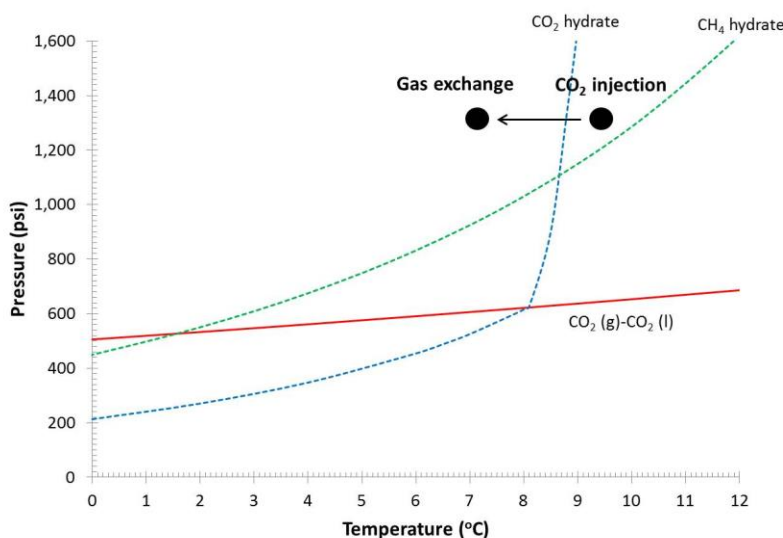
Figure 23: Hydrate phase boundary in CaCl$_2$ 5 wt% aqueous solution with description of experimental condition of liquid CO$_2$ injection.

Subtask 4.3 Data Exchange and Comparative Analysis of Gas Exchange Rates at Various Conditions

Nothing to report during this activity period.

Reference:

[1] Choi, J.H., Dai, S., Cha, J.H., and Seol, Y., "Laboratory Formation of Noncementing Hydrates in Sandy Sediments," published in *Geochemistry, Geophysics, Geosystems*, DOI: 10.1002/2014GC005287, p 15, 2014.

Changes in Approach:

The team is focusing on CO_2 gas injection with higher S_W condition rather than (CO_2+N_2) mixed gas system.

Problems or Delays:

The exchange mechanism is delayed due to a SARS issue on the Raman laser.

Exchange kinetics are delayed because the experimental procedure needs to be modified to avoid undesirable hydrate formation from free water during the gas exchange process

Changes in Key Personnel and Partnerships:

Nothing to report during this activity period.

Technology Transfer Activities or Product Produced:

Nothing to report during this activity period.

Task 5.0 Pore Scale Visualization and Characterization of Hydrate-Bearing Sediments

Objective

The objective of this task includes: (1) visualizing pore spaces within lab-synthesized hydrate-bearing sediments of cementing or non-cementing habits, (2) obtaining high resolution CT images of pore space hydrates, (3) performing grain-scale modeling of fluid flow using the 3D models developed based on the high resolution CT images, and (4) developing insight into how hydrate pore habits in pore space impacts potential gas production.

Scope of Work

Laboratory formed hydrate-bearing samples will be subjected to high resolution x-ray CT imaging. The NETL high resolution micro-XCT scanner will be used to obtain micron-scale voxel resolution images of hydrate-bearing samples and capture pore scale phenomenon. A pressure-temperature control system built around the CT scanner will be connected to the beryllium pressure vessel, where hydrate samples will be formed for fluid injection, gas exchange, and hydrate aging experiments.

Accomplishments this Period:

Subtask 5.1 Pore Scale Visualization of Hydrate Bearing Sediments with High Resolution X-ray CT Scanners

Analogue studies using specimens made of fine sand (F110) and polyurethane powder (density $\rho = 0.9g/cm^3$, closest to the density of methane hydrate) mixtures, have been scanned with the high resolution x-ray CT scanner. Through trial-and-error, the following parameters provided the best image quality: source-sample-distance $SSD = 50mm$; detector-sample-distance $DSD = 30mm$; voltage $V = 80keV$; lens magnification 10x or 20x (Figure 24).

| (a) | (b) | (c) |
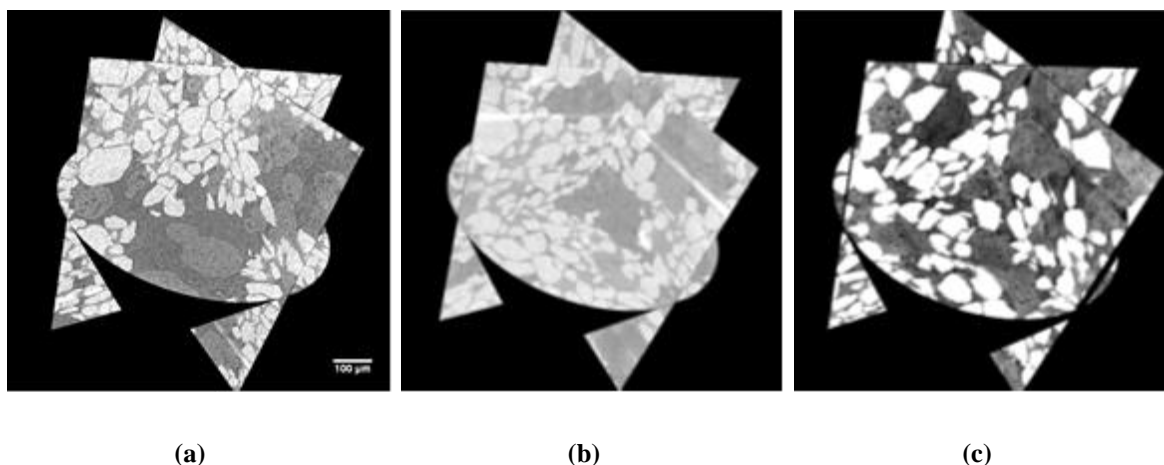
Figure 24: Micro-XCT scans of analogue specimen: sand and plastic mixture (resolution: 0.592μm). (a) Dry specimen without a core holder. (b) Water-saturated specimen in aluminum core holder. (c) Water-saturated specimen in beryllium core holder: results show much better contrast with less noise among different materials.

A specimen scanned at different energy levels has slightly different distributions in gray scales. When the scanning voltage exceeds ~100KeV, the main X-ray absorption mechanism alters from photoelectric effect to Compton scattering. Average of images scanned at two energy levels (one above 100KeV and one below 100KeV) provides better material contrast and low image noise (Figure 25).

| (a) | (b) |
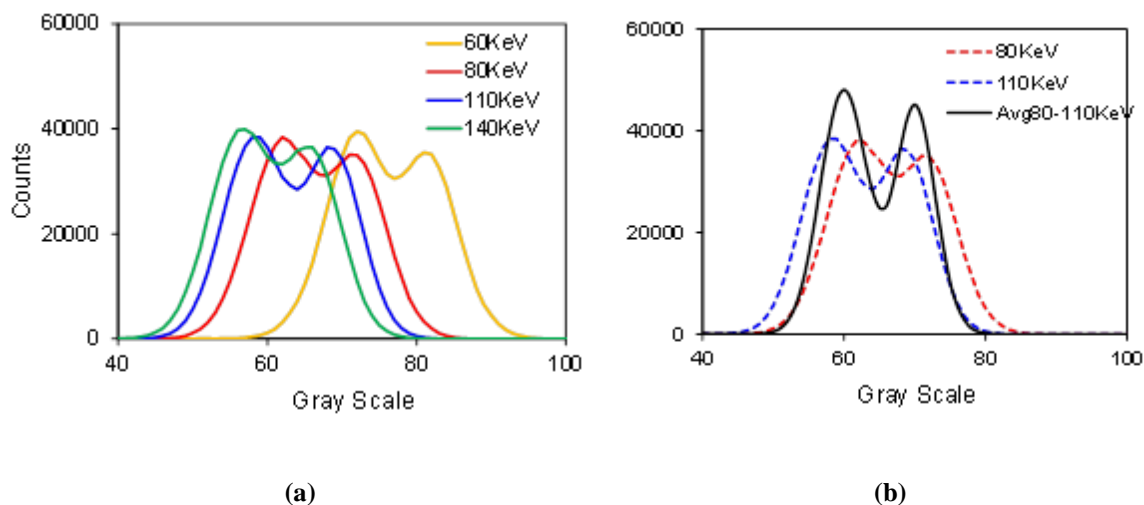
Figure 25: Gray scale distribution of analogue specimen. (a) Gray scale distribution obtained under four different scanning energy levels. (b) Gray scale distribution of averaged images from two scanning energy levels has much sharper contrast with less noise scattering.

Subtask 5.2 Grain Scale Constitutive Modeling for Hydrate Bearing Sediments

Effects of hydrate pore habits:

Figure 26 summarizes the reduction in water permeability due to an increase in hydrate saturation in capillary tubes with different cross sectional shapes, together with the Tokyo model using two *N* values (i.e., 1 and 10). The Tokyo model became identical to the grain-coating circular capillary tube model when *N* = 2. In general, pore-filling hydrate reduces the water permeability more significantly than grain-coating hydrate; which reflects the more inherent slow water conductance in annulus flow than pipe flow due to surface friction (i.e., annulus flow has more fluid-wall area). Water permeability reductions, due to increased hydrate saturation using capillary tube models, vary dramatically and the results obtained are too broad to be useful. For instance, to decrease the relative water permeability to one tenth of its original value (i.e., water permeability in hydrate free sediments), the pore-filling simple cubic packing tube model requires a hydrate saturation of S_h = ~0.1, while the grain-coating simple cubic packing model (with capillary effect) requires S_h = ~0.8 [refer to Figure 26(b)]. Capillary tube models use a bundle of parallel tubes to represent the pore structure of sediments and implicitly assume hydrate nucleates and identical saturation in each tube. These assumptions fail to capture the innate heterogeneous hydrate distribution in natural sediments, as described in the following section.

(a)

(b)
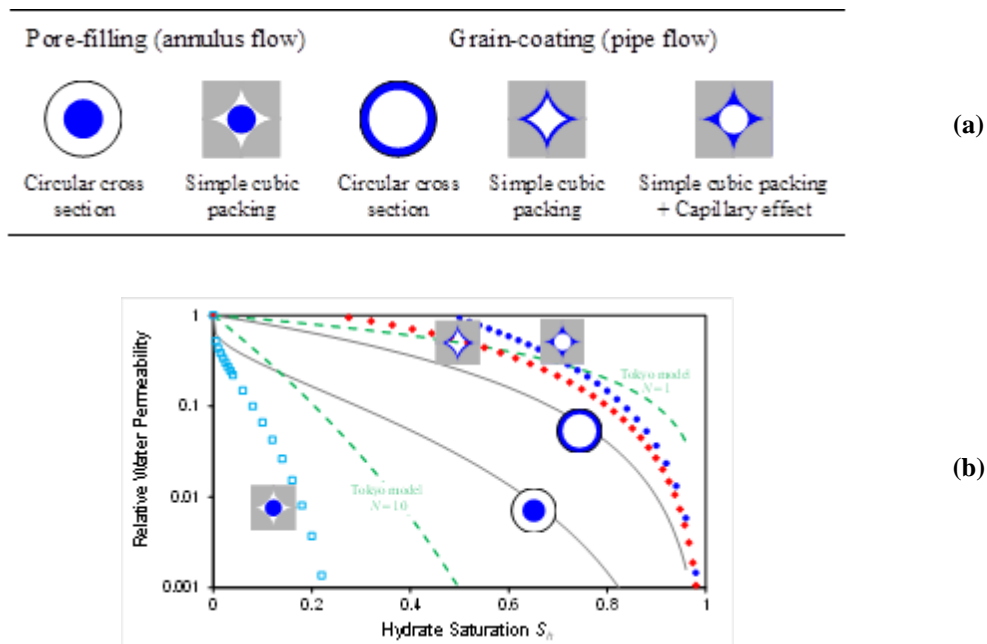
Figure 26: (a) Comparison of types of pore-filling hydrates and (b) relative permeability depending on the type of hydrate filling pores.

Heterogeneous hydrate distribution:

Figure 27 shows hydrate distribution within the network, according to the five different hydrate accumulation habits, for an identical hydrate saturation S_h = 0.2. These preferential accumulations of hydrates in sediments resulted in various effects on water permeability reduction due to increased hydrate saturation. The Min- and Max-case provided two bounds on the k_r-S_h relationship: larger clusters (C3) lower the water permeability more effectively than smaller

clusters (C1). Results agree with FEM simulations [1], which show that hydraulic conductivity is smaller when hydrate patch size is larger at identical total hydrate saturation.
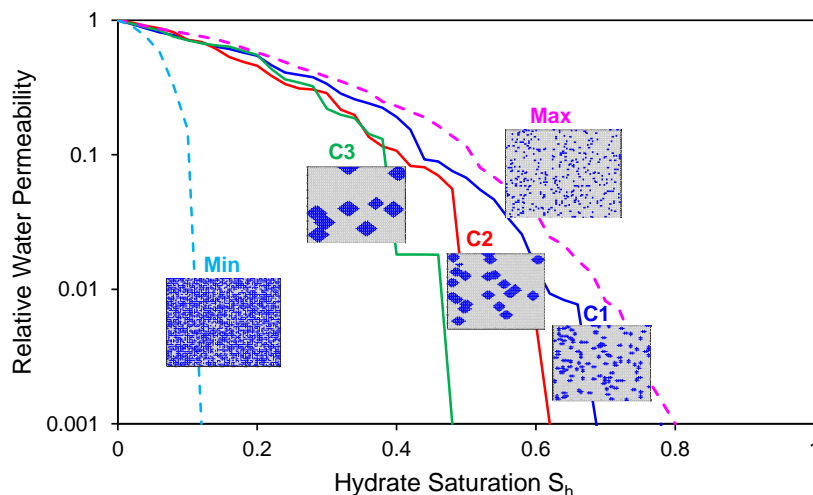
Figure 27: Preferential hydrate nucleation in the largest (Max) or smallest (Min) pores.

Semi-empirical water permeability (kAWP) – hydrate saturation (Sh) relationship:

Hydrate nucleation in sediments slows the fluid flow by decreasing sediment porosity and increasing hydraulic tortuosity. These effects were investigated using pore network modeling simulations and considered different hydrate saturations, distributions, and patch sizes. Results permitted the modification of the Kozeny-Carman equation to characterize fluid flow in hydrate bearing sediments: $k_r = (1 - S_h)^3 / (1 + 2S_h)^2$, which agrees well with limited laboratory/field measurements (Figure 28). This model captured flow physics and was easily incorporated into numerical simulators to study flow behaviors of hydrate bearing sediments.

$$k_r = \frac{k_{AWP}}{k_0} = \frac{(1 - S_h)^3}{(1 + 2S_h)^2}$$
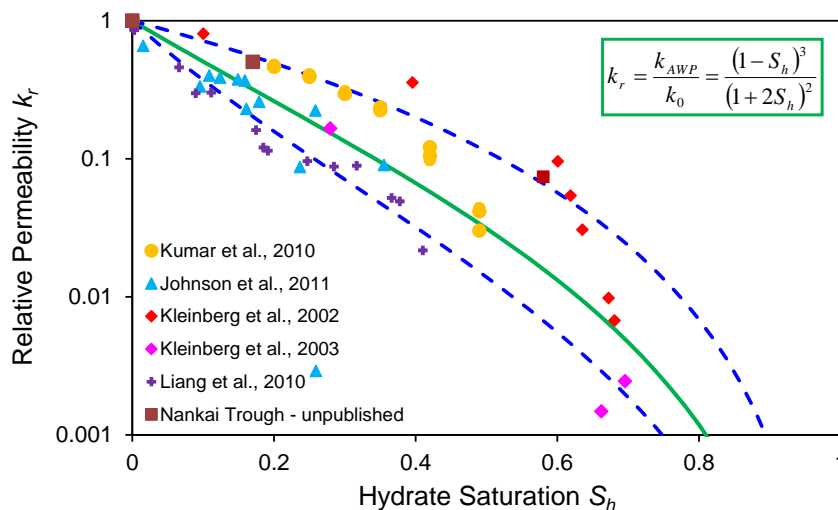
Figure 28: Relative permeability with varied hydrate saturation predicted based on pore network modeling investigation on hydrate effects to flow tortuosity and sediment specific surface, semi-empirical Kozeny-Carman equation.

Reference:

[1] Dai, S., Santamarina, J.C., Waite, W.F., and Kneafsey, T.J., "Hydrate morphology: Physical Properties of Sands with Patchy Hydrate Saturation," *Journal of Geophysical Research: Solid Earth (1978–2012)*, p 117 (B11), 2012.

Changes in Approach:

Nothing to report during this activity period.

Problems or Delays:

Nothing to report during this activity period.

Changes in Key Personnel and Partnerships:

Nothing to report during this activity period.

Technology Transfer Activities or Product Produced:

Dai, S., and Seol, Y., "Water Permeability in Hydrate Bearing Sediments: A Pore-scale Study," submitted for publication to the *Geophysical Research Letter*, 2014.

4.0 Risk Analysis

Potential risks were identified as per the Project Risk Register in the PMP. All other risks noted in the register remained in force as originally identified. No new risks to project success were identified.

5.0 Milestone Status

The status of each major milestone is shown below in Table 2: Natural Gas Hydrates Research Support Milestone Status

Milestone Identifier	Title	Planned Date	Actual/ Forecast Completion	Milestone Status	Activities Driving Milestone	Activity Percent Complete	Comments/ Variance Analysis
Task 2.0 Reservoir Simulation of Gas Hydrates Production Field Tests							
M1.14.2.A	Development and distribution of elementary problem sets for code comparison study.	12/31/13	03/31/14	**Completed**		100%	None
M1.14.2.B	Development and distribution of Iġnik Sikumi-based problem sets for code comparison study.	04/30/14	04/30/14	**In progress**		85%	None
M1.14.2.C	Complete simulations of production and flow modeling representative of a long-term depressurization test and modeling-based assessment of the potential for methane production from CO_2/N_2 exchange test.	06/30/14	06/30/14	**In progress**		25%	

Milestone Identifier	Title	Planned Date	Actual/ Forecast Completion	Milestone Status	Activities Driving Milestone	Activity Percent Complete	Comments/ Variance Analysis
Task 3.0 Developing Constitutive Models of Various Hydrate-Bearing Sands							
M1.14.3.A	Complete tri-axial geomechanical strength and deformability tests on CH_4 and CO_2-hydrate bearing sediments.	03/31/14	06/30/14	**Delayed**		25%	None
M1.14.3.B	Complete data analysis for tri-axial tests and development of a constitutive model defining the relationship between hydrate saturation and elastoplastic soil behavior parameters.	09/30/14	09/30/14	**In progress**		60%	None
Task 4.0 Assessment of Gas Exchange Processes of CH_4 Hydrate with CO_2 under Reservoir Conditions							
M1.14.4.A	Complete CO_2 (and/or CO_2/N_2 mixture) - CH_4 gas exchange mechanism tests with Raman spectroscopy.	03/31/14	06/30/14	**Delayed**		20%	None
M1.14.4.B	Complete the measurements of CO_2 (and/or CO_2/N_2 mixture) - CH_4 exchange kinetics with the presence of free water.	03/31/14	06/30/14	**Delayed**		25%	None
M1.14.4.C	Complete comparative analysis for gas exchange kinetics data from experiments conducted at: NETL, LBNL, and PNNL (if available).	06/30/14	06/30/14	**In progress**		0%	None
5.0 Pore Scale Visualization and Characterization of Hydrate-Bearing Sediments							
M1.14.5.A	Complete development of pore scale imaging procedures and collection of hydrate images of hydrate-bearing sediments.	03/31/14	03/31/14	**Completed**		100%	None
M1.14.5.B	Complete development of grain scale constitutive models for hydrate-bearing sediments based on CT images.	09/30/14	09/30/14	**In progress**		25%	None

Milestone Identifier	Title	Planned Date	Actual/ Forecast Completion	Milestone Status	Activities Driving Milestone	Activity Percent Complete	Comments/ Variance Analysis
Milestone Status Key:							
Blue = Complete							
Green = Forecast Date is equal to or less than the planned completion							
Yellow = Forecast Date is greater than the planned completion by 1 to 30 days							
Red = Forecast Date is greater than the planned completion date by more than 30 days							

. Planned and actual milestone due dates have been revised to match the active Project Management Plan (PMP).

Table 2: Natural Gas Hydrates Research Support Milestone Status

Milestone Identifier	Title	Planned Date	Actual/ Forecast Completion	Milestone Status	Activities Driving Milestone	Activity Percent Complete	Comments/ Variance Analysis
Task 2.0 Reservoir Simulation of Gas Hydrates Production Field Tests							
M1.14.2.A	Development and distribution of elementary problem sets for code comparison study.	12/31/13	03/31/14	**Completed**		100%	None
M1.14.2.B	Development and distribution of Iġnik Sikumi-based problem sets for code comparison study.	04/30/14	04/30/14	**In progress**		85%	None
M1.14.2.C	Complete simulations of production and flow modeling representative of a long-term depressurization test and modeling-based assessment of the potential for methane production from CO_2/N_2 exchange test.	06/30/14	06/30/14	**In progress**		25%	
Task 3.0 Developing Constitutive Models of Various Hydrate-Bearing Sands							
M1.14.3.A	Complete tri-axial geomechanical strength and deformability tests on CH_4 and CO_2-hydrate bearing sediments.	03/31/14	06/30/14	**Delayed**		25%	None
M1.14.3.B	Complete data analysis for tri-axial tests and development of a constitutive model defining the relationship between hydrate saturation and elastoplastic soil behavior parameters.	09/30/14	09/30/14	**In progress**		60%	None
Task 4.0 Assessment of Gas Exchange Processes of CH_4 Hydrate with CO_2 under Reservoir Conditions							
M1.14.4.A	Complete CO_2 (and/or CO_2/N_2 mixture) - CH_4 gas exchange mechanism tests with Raman spectroscopy.	03/31/14	06/30/14	**Delayed**		20%	None
M1.14.4.B	Complete the measurements of CO_2 (and/or CO_2/N_2 mixture) - CH_4 exchange kinetics with the presence of free water.	03/31/14	06/30/14	**Delayed**		25%	None

Milestone Identifier	Title	Planned Date	Actual/ Forecast Completion	Milestone Status	Activities Driving Milestone	Activity Percent Complete	Comments/ Variance Analysis
M1.14.4.C	Complete comparative analysis for gas exchange kinetics data from experiments conducted at: NETL, LBNL, and PNNL (if available).	06/30/14	06/30/14	**In progress**		0%	None
5.0 Pore Scale Visualization and Characterization of Hydrate-Bearing Sediments							
M1.14.5.A	Complete development of pore scale imaging procedures and collection of hydrate images of hydrate-bearing sediments.	03/31/14	03/31/14	**Completed**		100%	None
M1.14.5.B	Complete development of grain scale constitutive models for hydrate-bearing sediments based on CT images.	09/30/14	09/30/14	**In progress**		25%	None
Milestone Status Key:							
Blue = Complete							
Green = Forecast Date is equal to or less than the planned completion							
Yellow = Forecast Date is greater than the planned completion by 1 to 30 days							
Red = Forecast Date is greater than the planned completion date by more than 30 days							

6.0   Schedule Status

Specific schedule issues are discussed by task and subtask in the Technical Highlights Section.

Design and fabrication of beryllium core holders has been delayed due to the slow progress of PE review on the design. New scheduled delivery for the vessel has not been determined.

7.0   Budget and Cost Status

The budget (plan) for the FY14-Q2 was $153K while the actual cost was $106K, resulting in a cost variance of $46K (rounded values). Cumulative to date, the budget (plan) was $269K while the actual cost was $150K, resulting in a cost variance of $119K. This variance, attributed to under runs within the RES contract (subcontracts/ODCs) and DOE portions of the FWP, will be expended before the end of the Period of Performance.

Figure 29 below and Table 3 and Table 4 in Appendix A show detailed cost information for FY14.

NATURAL GAS HYDRATES PROGRAM COST PERFORMANCE HISTOGRAM

	FY14 - Q1	FY14 - Q2	FY14 - Q3	FY14 - Q4	TOTAL
Period					
Plan	$117	$153	$157	$199	$625
Actual	$43	$106			$150
Cumulative					
Plan	$117	$269	$426	$625	$625
Actual	$43	$150			$150
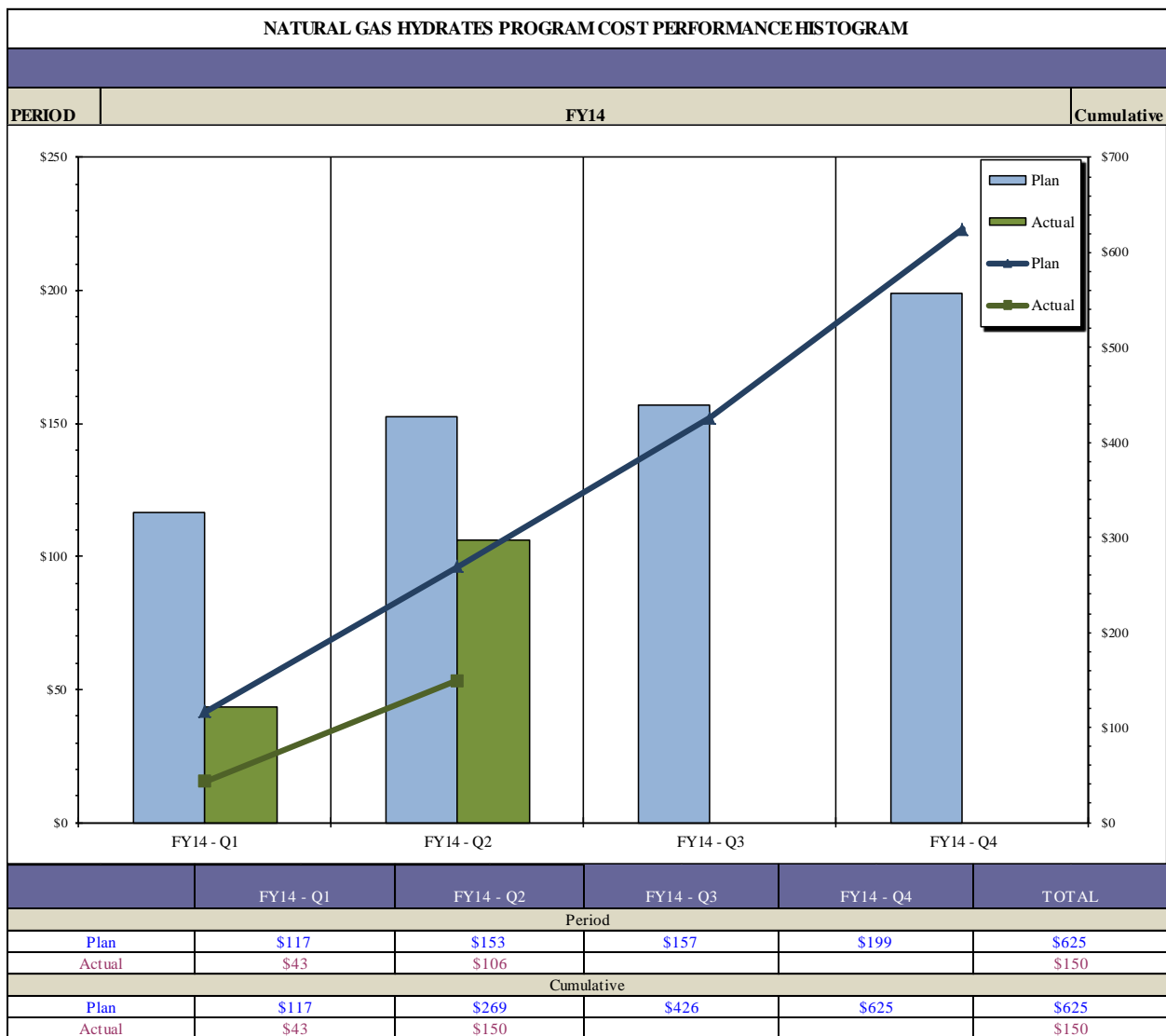
Figure 29: Natural Gas Hydrates Research cost performance histogram ($ x 1,000).

8.0   References

References are listed in Sections 1.0 and 3.0 of this report.

Appendix A: **Budget and Cost Status**

Table 3: Natural Gas Hydrate Research Field Work Proposal Budget Status (Current Period)

DOLLARS IN THOUSANDS													
CURRENT PERIOD													
Title	WBS	PLAN FY14 - Q1	ACTUAL FY14 - Q1	VAR FY14 - Q1	PLAN FY14 - Q2	ACTUAL FY14 - Q2	VAR FY14 - Q2	PLAN FY14 - Q3	ACTUAL FY14 - Q3	VAR FY14 - Q3	PLAN FY14 - Q4	ACTUAL FY14 - Q4	VAR FY14 - Q4
Project Management and Outreach	1	$2	$3	($1)	$2	$3	($1)	$2			$2		
Reservoir Simulation of Gas Hydrates Production Field Tests	2	$18	$0	$18	$20	$14	$6	$30			$96		
Developing Constitutive Models of Various Hydrate-Bearing Sands	3	$27	$0	$27	$27	$36	($9)	$51			$27		
Assessment of Gas Exchange Processes of CH4 Hydrate with CO2 under Reservoir Conditions	4	$21	$16	$5	$54	$24	$31	$23			$21		
Pore Scale Visualization and Characterization of Hydrate-Bearing Sediments	5	$23	$0	$23	$23	$0	$23	$23			$23		
ORD OH		$24	$24	$0	$24	$24	$0	$24			$24		
Fee		$2	$0	$2	$2	$5	($2)	$5			$7		
Total		$117	$43	$73	$153	$106	$46	$157			$199		

Includes costs for general infrastructure support.

Table 4: Natural Gas Hydrate Research Field Work Proposal Budget Status (Cumulative)

		DOLLARS IN THOUSANDS											
		CUMULATIVE											
Title	WBS	PLAN FY14 - Q1	ACTUAL FY14 - Q1	VAR FY14 - Q1	PLAN FY14 - Q2	ACTUAL FY14 - Q2	VAR FY14 - Q2	PLAN FY14 - Q3	ACTUAL FY14 - Q3	VAR FY14 - Q3	PLAN FY14 - Q4	ACTUAL FY14 - Q4	VAR FY14 - Q4
Project Management and Outreach	1	$2	$3	($1)	$4	$6	($2)	$6			$8		
Reservoir Simulation of Gas Hydrates Production Field Tests	2	$18	$0	$18	$38	$14	$24	$67			$163		
Developing Constitutive Models of Various Hydrate-Bearing Sands	3	$27	$0	$27	$53	$36	$17	$104			$130		
Assessment of Gas Exchange Processes of CH4 Hydrate with CO2 under Reservoir Conditions	4	$21	$16	$5	$75	$40	$35	$99			$119		
Pore Scale Visualization and Characterization of Hydrate-Bearing Sediments	5	$23	$0	$23	$45	$0	$45	$68			$91		
ORD OH		$24	$24	$0	$49	$49	$0	$73			$98		
Fee		$2	$0	$2	$5	$5	($0)	$9			$16		
Total		$117	$43	$73	$269	$150	$119	$426			$625		

Includes costs for general infrastructure support.